2007-24-0046
SAND2007-5634C

Experimental Assessment of Reynolds-Averaged Dissipation Modeling in Engine Flows

Paul C. Miles
Sandia National Laboratories, Livermore, CA

Bret H. RempelEwert and Rolf D. Reitz
Engine Research Center, University of Wisconsin, Madison, WI

ABSTRACT

The influence of the constant C_3, which multiplies the mean flow divergence term in the model equation for the turbulent kinetic energy dissipation, is examined in a motored diesel engine for three different swirl ratios and three different spatial locations. Predicted temporal histories of turbulence energy and its dissipation are compared with experimentally-derived estimates. A "best-fit" value of $C_3 = 1.75$, with an approximate uncertainty of ±0.3 is found to minimize the error between the model predictions and the experiments.

Using this best-fit value, model length scale behavior corresponds well with that of measured velocity-correlation integral scales during compression. During expansion, the model scale grows too rapidly. Restriction of the model assessment to the expansion stroke suggests that $C_3 = 0.9$ is more appropriate during this period.

INTRODUCTION

The k-ε turbulence model has been the mainstay of flow modeling in reciprocating engines for the last three decades. Although other methods with important advantages (notably large-eddy simulation techniques) are becoming more viable as computing power increases, the k-ε model is likely to remain widely used for repetitive engine design and optimization calculations for many years. Within this model, the influence of turbulence on the mean flow development is modeled through use of a turbulent viscosity ν_T which is added to the molecular viscosity in the momentum equations. The turbulent viscosity is computed from the turbulent kinetic energy k and its rate of dissipation ε using the relation

$$\nu_T = C_\mu k^2 / \varepsilon \tag{1}$$

where k and ε are obtained from the conservation equations

$$\frac{Dk}{Dt} = \mathcal{P} - \varepsilon + Diffusion \tag{2}$$

and

$$\frac{D\varepsilon}{Dt} = \frac{\varepsilon}{k}\left(C_1\mathcal{P} - C_2\varepsilon\right) + \left(1 - C_3\right)\varepsilon\left(\nabla \cdot \mathbf{U}\right) + Diffusion \tag{3}$$

C_μ, C_1, C_2, and C_3 are model constants, and the production of turbulent kinetic energy $\mathcal{P}$ is given by

$$\mathcal{P} = -u_i u_j S_{ij} \tag{4}$$

The k-ε equations are closed by introduction of a simple linear relationship for the deviatoric part of the turbulent stresses

$$u_i u_j - \frac{2}{3}k\delta_{ij} = -2\nu_T\left(S_{ij} - \frac{1}{3}\left(\nabla \cdot \mathbf{U}\right)\delta_{ij}\right) \tag{5}$$

and by well-accepted approximations for the diffusion terms.

Despite its long use in engine flow simulations, considerable uncertainty remains regarding the application of the k-ε model to flows with bulk compression. Appropriate modifications to the ε–equation, in particular selection of the model constant C_3, have not been clearly established. The importance of choosing an appropriate value of C_3 is not disputed, however. The impact on the simulated turbulence field of various proposed values for C_3 has been examined in several studies [4,9,11,14,24]. For low levels of turbulence energy at the start of compression, predicted near-TDC turbulence energy can differ by more than an order of magnitude for different values of C_3, while with more typical initial turbulence levels 2–3 fold changes in turbulence energy near TDC are observed. Still larger changes are seen in the variation of the modeled turbulent time or length scales, which can evolve in qualitatively dissimilar manners for differing values of C_3.

There is very little experimental or numerical evidence to support the choice of one value of C_3 over another. Although direct measurements of the dissipation rate in a motored engine have been achieved [12], no information pertinent to the selection of C_3 can be derived from the data reported. Previous attempts to assess the dissipation modeling have relied heavily on measurements of the velocity-correlation length scale ℓ and compared its temporal variation to that of the model (or dissipation) length scale $\ell_\varepsilon \approx k^{3/2}/\varepsilon$. Numerous measurements of ℓ have been reported and are reviewed in [13]. The bulk of these measurements suggest that ℓ reaches a broad minimum near TDC—a result which is also physically appealing. Early work aimed at identifying an appropriate value for C_3 compared the predicted evolution of ℓ_ε directly to the measured (or expected) evolution [4,9,14,15]. Of these studies, that of Ikegami *et al.* [14] is notable in that they compare the modeled and measured evolution of both ℓ_ε and k, and recommend a specific value $C_3 = 1.7$ during compression.

More recent efforts, acting on Coleman and Mansour's [8] observation that ℓ_ε and ℓ cannot—in general—be expected to be proportional, have employed the scaling relation $\ell_\varepsilon \propto \ell \mathrm{Re}_\ell$ to compare the evolution of the model and experimental length scales [10,16,17]. This relation relies on the rapid distortion theory result that that the ratio of the Taylor scale λ to ℓ remains constant under rapid spherical compression (Wu, *et al.* [18]). Studies performed in motored engines [10,16] found better qualitative agreement between measured integral scales and model scales when this alternative scaling relation is employed. Length scale comparisons made in flows with fuel injection [17], however, found no advantage to using this scaling relation.

Assessments of dissipation modeling have also been made through comparison of the model predictions with the results of direct numerical simulations (DNS). This approach was pursued by Wu *et al.* [18] and later by Coleman and Mansour [8, 20]. Wu *et al.* found that for rapid compression, the modeled dissipation equation could not adequately predict the dissipation calculated via DNS. Coleman and Mansour, however, showed that by properly accounting for viscosity variation the DNS results could be accurately replicated by the model equation using a value for C_3 derived from rapid distortion theory. Wu *et al.* also investigated compression rates appropriate to engine flows, where the ratio η of turbulent time scale k/ε to mean flow time scale $S^{-1} = \sqrt{S_{ij}S_{ij}}^{-1}$ is of order unity. The model ε equation again failed to predict the DNS results, which indicated that for spherical compression the true dissipation rate lay between the rates predicted with $C_3 = 0$ and $C_3 = (7\text{-}2C_1)/3$. No attempt to find an optimal value for C_3 was reported.

One-dimensional compression of turbulence was also investigated by Wu *et al*. In this case, the model could predict neither k nor ε correctly, due to the need to invoke Eq. 5 to predict $\mathcal{P}$. Because the modeling of both $\mathcal{P}$ and ε were error prone, no identification of an appropriate value for C_3 was attempted.

The present work employs an alternative, experimentally-based approach to identify appropriate values for the constant C_3. Rather than rely primarily on a comparison of length scale evolution to assess the influence of C_3, this approach minimizes the error between the model predictions, the measured evolution of k, and an indirect measure of ε. An important feature of this approach is the use of (primarily) experimentally-derived estimates of $\mathcal{P}$, thereby minimizing the sensitivity of the results to errors incurred through the use of Eq. 5. The model results obtained are further examined by comparison of the evolution of ℓ_ε with ℓ and with $\ell\mathrm{Re}_\ell$ to identify values of C_3 resulting in physically plausible behavior.

ADDITIONAL BACKGROUND

OVERVIEW OF PROPOSED VALUES FOR C_3

Commonly used values for C_3, and a sampling of the workers who have proposed, recommended, or used these values, are tabulated in Table 1. Early IC engine computations either used a value of C_3 obtained from terms appearing in a direct derivation of the ε transport equation [1], from rapid-distortion analysis [2], or from application of the constant-density formulation of the modeled ε equation [3]. The second approach was later extended to allow for various forms of compression: isotropic (spherical), unidirectional, or axisymmetric (cylindrical-radial) [4].

For low Mach number flows the fluctuation velocity is divergence-free and only the solenoidal part of the dissipation need be considered, $\varepsilon \approx \nu\langle\omega_i\omega_i\rangle$. Changes in dissipation can thus be achieved by changing the fluctuating vorticity (ω_i) field at constant molecular viscosity or by changing the viscosity without altering the dissipative flow structures. Based on a detailed order-of-magnitude analysis of the various terms in the exact ε transport equation, El Tahry [5] identified the importance of including the effect of varying viscosity in the model equation, though he modeled this effect separately and did not specifically include it in his expression for C_3. Coleman and Mansour [8] derived rapid-distortion expressions for the rate-of-change of k and $\langle\omega_i\omega_i\rangle$ under isotropic compression, and equated these expressions to the modeled equations. Their result also retains a term associated with changes in viscosity. In performing this analysis, Coleman and Mansour avoided the assumptions of previous work ([2], [4]) that the model (or dissipation) length scale ℓ_ε is proportional to the velocity-correlation integral scale ℓ. This assumption can be expected to be valid only when the turbulence is in equilibrium (such that the energy dissipation rate equals the rate at which turbulence energy is transferred in the energy cascade) or, as demonstrated by Coleman and Mansour, when the viscosity remains constant. The work

Table 1 A brief history of the constant C_3

C_3	Workers (Year) [Reference]
0	Gosman, Johns, & Watkins (1980) [1]
$\frac{(7-2C_1)}{3}$ {1.37}	Reynolds (1980) [2]
1	Ramos & Sirignano (1980) [3]
$\frac{(7-2C_1)}{3} \rightarrow \frac{(8-2C_1)}{3}$ {1.37 ➔ 1.71}	Morel & Mansour (1982) [4] (strain field dependent)
$\frac{7}{3} - \frac{1}{(\nabla\cdot\mathbf{U})}\frac{1}{\nu}\frac{d\nu}{dt}$ {1.58}	El Tahry (1983) [5]
2	Grasso and Bracco (1983) [6] Amsden, O'Rourke, & Butler (1989) [7]
$\frac{(7-2C_1)}{3} - \frac{1}{(\nabla\cdot\mathbf{U})}\frac{1}{\nu}\frac{d\nu}{dt}$ {0.62}	Coleman & Mansour (1991) [8]
$\frac{(7-2C_1)}{3} - f(\eta) - \frac{1}{(\nabla\cdot\mathbf{U})}\frac{1}{\nu}\frac{d\nu}{dt}$ {0.62 – $f(\eta)$}	Han & Reitz (1996) [9]
$3 - \frac{1}{(\nabla\cdot\mathbf{U})}\frac{1}{\nu}\frac{d\nu}{dt}$ {2.25}	Bianchi, Michelassi, & Reitz (1999) [10]

Numerical values given in { } are calculated with C_1 = 1.44 and using Eq. 6 with m = 0.69 and γ = 1.36

of Coleman & Mansour has now been extended to the case of unidirectional compression by Bianchi and co-workers [10].

Han and Reitz [9] followed a similar rapid-distortion analysis based on isotropic compression, but started with a modeled form for the ε equation that included a term dependent on the characteristic turbulent to mean flow time scale ratio $\eta = Sk/\varepsilon$. This term, which is a function of the magnitude of the applied strain, is designed to increase the dissipation rate in regions of high strain. As a result of their inclusion of this term, C_3 is also dependent on η.

THE INFLUENCE OF MOLECULAR VISCOSITY

As shown in Table 1, many of the more recent studies have incorporated the change in molecular viscosity ν in their modeling of the influence of compression on the turbulent energy dissipation. For isentropic compression with a specific heat ratio γ and $\mu \propto T^m$, El Tahry observed that

$$\frac{1}{(\nabla\cdot\mathbf{U})}\frac{1}{\nu}\frac{d\nu}{dt} = 1 - m(\gamma - 1), \qquad (6)$$

an expression which is approximately constant as temperature and pressure vary. Hence, most researchers have incorporated the influence of viscosity changes into C_3. Eq. 6 was obtained using the relation $1/\rho\ d\rho/dt = -\nabla\cdot\mathbf{U}$, valid when $\nabla\rho = 0$. In applications, the rate of change of viscosity can be evaluated directly and it is not necessary to assume a constant value for Eq. 6. However, it is convenient to make this assumption for the purpose of comparing the various expressions in Table 1 to the values of C_3 obtained from the experiments discussed below. For air, $m \approx 0.69$ over the temperature range of 300–1000K, and γ varies from approximately 1.40–1.34. In the ±60°CA range about TDC examined below, $\gamma \approx 1.36$ and $1 - m(\gamma - 1)$ is taken equal to 0.75.

EXPERIMENT, SIMULATION, AND DATA ANALYSIS

The methodology for estimating an appropriate value of C_3 relies on the experimental determination of the evolution of k, and on estimates of $\mathcal{P}$ derived from both experimental data and numerical simulation. The experimental data were obtained using a two-component laser Doppler velocimeter to simultaneously measure the tangential and radial components of velocity in a swirl-supported diesel engine typical of automotive applications. The basic engine geometry and operating conditions employed are described in Table 2, while the measurement locations (with the piston depicted at TDC), bowl geometry, and coordinate system employed are shown in Figure 1. Measurements were made in clusters, centered about the same radial coordinate

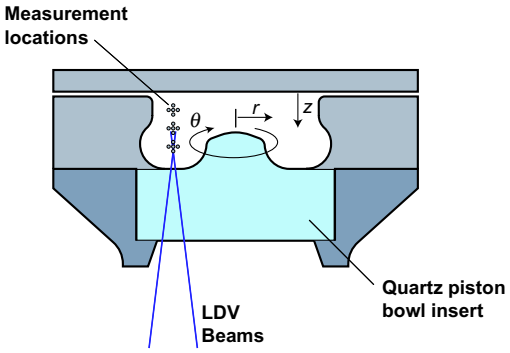

Figure 1. Piston bowl geometry showing the measurement locations and the cylindrical coordinate system employed in this work

r = 13.6 mm at axial distances z of 4, 8, and 12 mm below the cylinder head. Mean velocity gradients in the axial and radial directions can be determined directly from the measurements. Gradients in the tangential direction are assumed zero in this axisymmetric, motored flow.

The turbulence energy is approximated by

$$k = \frac{3}{4}\left(u_r'^2 + u_\theta'^2\right) \tag{7}$$

and turbulence production associated with bulk compression of the isotropic part of the normal stresses

$$\mathcal{P}_{iso} = -\frac{2}{3}k\left(\nabla\cdot\mathbf{U}\right) \tag{8}$$

can be calculated if $\nabla\cdot\mathbf{U}$ is known. $\mathcal{P}_{iso}$ has been shown to be the dominant turbulence production term in these flows [19]. Because only two of the three normal components of the mean strain rate tensor are measured, $\nabla\cdot\mathbf{U}$ cannot be determined directly from the data and must be estimated by other means. Neglecting blowby, and assuming a spatially-uniform density, $\nabla\cdot\mathbf{U}$ is given by *(1/V) dV/dt*—where V denotes the cylinder volume. Both blowby and excessive mass in cold boundary layers can invalidate this relationship, and it is instructive to evaluate other methods for estimating $\nabla\cdot\mathbf{U}$. Assuming that the bulk gases undergo an isentropic compression process (and that *local* density gradients are negligible), $\nabla\cdot\mathbf{U}$ can also be approximated from the measured pressure record as

$$\nabla\cdot\mathbf{U} \cong -\frac{1}{P^{1/\gamma}}\frac{dP^{1/\gamma}}{dt} \tag{9}$$

Estimates of $\nabla\cdot\mathbf{U}$ obtained with Eq. 9, accounting for a temperature-dependent specific heat ratio, are closely comparable to estimates obtained from *(1/V) dV/dt*—as is demonstrated in Fig. 2. Since analysis of selected operating conditions, with $\nabla\cdot\mathbf{U}$ obtained from both expressions, resulted in very similar values for C_3 the expression *(1/V) dV/dt* is employed for convenience.

Table 2 Engine geometry and operating conditions

Engine Geometry:

Bore:	7.95 [cm]	Bowl lip diam.:	3.63 [cm]
Stroke:	8.50 [cm]	Bowl depth:	1.58 [cm]
Comp. ratio:	18.7	Squish height:	0.67 [cm]

Operating Conditions:

Engine Speed	1500	[rpm]
Mean Piston Speed S_p	4.25	[m s^{-1}]
Swirl Ratio (Ricardo)	1.5, 2.5, and 3.5	

The dominant source of turbulence due to production by the anisotropic stresses, $u_r u_\theta S_{r\theta}$, is obtained from the measured shear stress and measured r-θ component of the mean strain rate tensor $S_{r\theta}$. Production associated with the anisotropic part of the normal stresses is also known, although the anisotropic portion of $u_z'^2$ requires estimation via Eq. 5 (S_{zz} is known from the estimate of $\nabla\cdot\mathbf{U}$).

The remaining production terms also require various degrees of modeling. Eq. 5 is again employed, with the measured $S_{z\theta}$, to obtain $u_z u_\theta S_{z\theta}$. This term is the most significant of the terms that require modeling, though it is generally small compared to $\mathcal{P}_{iso}$ or $u_r u_\theta S_{r\theta}$. Because $U_{z,r}$ is not measured, a full cycle simulation was performed using the KIVA computer code [7] to obtain estimates of S_{rz}. To obtain a good match with the experimental measurements, the standard KIVA velocity field initialization was modified to permit initialization with axial profiles of measured tangential and radial velocities. Generally, very good agreement between the evolution of simulated and measured mean velocities and their gradients—in both magnitude and phasing—was obtained. The contribution to $\mathcal{P}$ from S_{rz}, with $u_r u_z$ estimated from Eq. 5, however, was usually negligible.

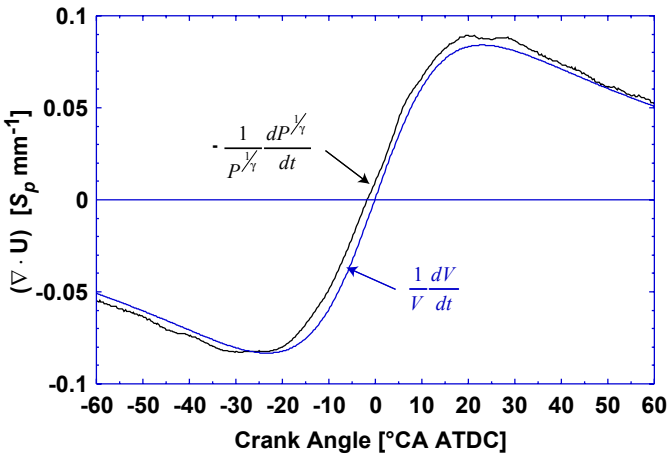

Figure 2. Estimates of $\nabla\cdot\mathbf{U}$ obtained by two different methods

Accurate modeling of this quantity is therefore of little consequence.

Longitudinal and lateral velocity-correlation length scales along the tangential direction, ℓ_f and ℓ_g, are also obtained from the data by applying Taylor's hypothesis. The ratio of fluctuating velocity to the mean tangential flow velocity, $(\frac{2}{3}k)^{\frac{1}{2}}/U_\theta$ lies in the range 0.1 – 0.5. Hence, the requirement that $(\frac{2}{3}k)^{\frac{1}{2}}/U_\theta << 1$ is not always valid, and the experimental length scales must be regarded as estimates. However, they are anticipated to exhibit qualitatively correct trends in their evolution. Length scales employed below are computed by a weighted average of the two measured length scales, scaled to approximate ℓ_g in magnitude:

$$\ell = \frac{1}{2}\left(\ell_g + \frac{\ell_f}{2}\right) \tag{10}$$

Additional details describing the magnitude and conditions under which the various production terms are of importance, as well as a more complete description of the experiment and data analysis procedures, can be found in [17] and [19].

METHODOLOGY FOR DETERMINING C_3

As discussed above, previous attempts to identify an appropriate value of C_3 have relied primarily on a comparison of the model length scale ℓ_ε with the measured integral scale ℓ. A pitfall of indirectly assessing dissipation modeling through comparison of length scales is that neither the linear relationship between ℓ and ℓ_ε (appropriate to equilibrium turbulence) nor the Re_ℓ-based scaling (appropriate to a large ratio of turbulent to mean flow time scale Sk/ε) is expected to be accurate.

Numerical simulations in a motored diesel engine with a re-entrant bowl geometry show that the volume-averaged $Sk/\varepsilon \approx 2$ during the 120°CA period centered on TDC [16†]. Estimates of the time-scale ratio obtained from the experimental data taken for this study, with ε estimated as described below, are consistent with the simulation results. Figure 3 presents the time scale ratios obtained at all measurement locations and swirl ratios. Sk/ε is found to remain within modest limits, between roughly 0.5 and 3.5.†† At these time scale ratios, the turbulence is neither in equilibrium nor is it being distorted with sufficient rapidity (or sphericity) that λ and ℓ can be expected to remain proportional. However, the two

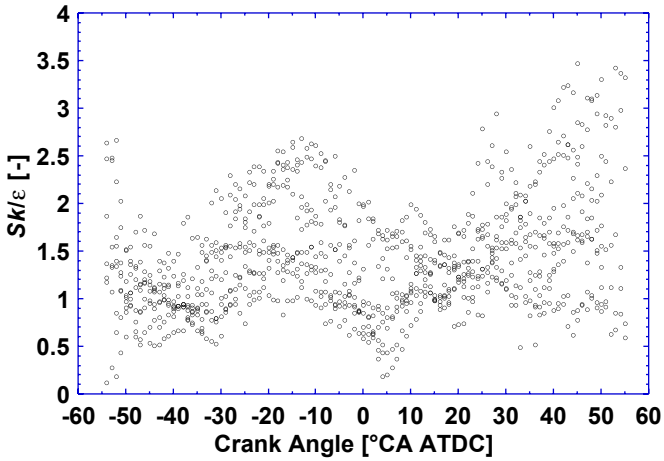

Figure 3. Turbulent to mean flow time scale ratios Sk/ε measured under motored operation for three different measurement locations and three swirl ratios. Note that these time scale ratios are all of order one

scaling relations do provide useful limits that can be employed to assess whether or not the model length scale exhibits plausible behavior. Note that the above cited range of time scale ratios is appropriate only for motored flows. For flows with fuel injection and combustion, much smaller mean flow time scales are likely to be attained.

An additional drawback associated with comparison of the modeled length scale to measured length scales is the limited experimental length scale information available. In non-isotropic engine flows several distinct turbulent length scales can be defined, which may exhibit quite different behavior (*e.g.* [15,17]).

Rather than rely on a comparison of the model and velocity-correlation length scales, here a "best-fit" value for C_3 is determined by minimizing the error between experimental and model-based estimates of k and ε in a ±50°CA window centered about TDC compression. Several key aspects to this determination should be noted:

1) In order to integrate Eqs. 2 and 3, $\mathcal{P}$ must be known. The key difference between this work and previous turbulence modeling assessments is the use of measured data to determine the dominant components of $\mathcal{P}$, as described above. Hence, the introduction of error in $\mathcal{P}$, associated with the use of Eq. 5 to model the anisotropic stresses, is greatly reduced.

2) Homogeneous turbulence is assumed. With this assumption, the convective terms and diffusive terms vanish in Eqs. 2 and 3. At low swirl ratios, and away from the bowl lip region, the production of turbulence is dominated by bulk compression of the isotropic part of the normal stresses, and an initially homogeneous turbulence field will remain approximately homogeneous—behavior which is

† In the cited study S is defined as $\sqrt{2S_{ij}S_{ij}}$

†† Between -30°CA and TDC, the broad maximum in Sk/ε is due to increased mean flow strain rates associated with the maximum in bulk compression rate due to piston motion (occurring near -25°CA) and the squish flow into the piston bowl (the peak squish velocity occurs near -15–-10°CA). Later in the expansion stroke, increased Sk/ε is due to an increase in the turbulent time scale.

observed experimentally [19]. Under these circumstances, the assumption of homogeneity is reasonably justified. At higher swirl ratios, the squish flow induces substantial departures from a solid-body-like flow structure and gradients in the swirl velocity become important sources of turbulence. In contrast to the low swirl flows, these flows are clearly not homogeneous. However, the main influence of inhomogeneity will be to cause the measured k and ε to oscillate about the smoother model predictions.

3) Fluid properties (ρ, T, μ) vary with time, but are assumed to be spatially uniform.

4) The "best-fit" value of C_3 is determined by minimizing the function

$$F = \sum \left(k_{meas} - k_{model}\right)^2 + W \sum \left(\varepsilon_{meas} - \varepsilon_{model}\right)^2 \qquad (11)$$

where the summation is over the crank angle range -50 to 50°CA ATDC, where data quality is best. The "measured" dissipation ε_{meas} is computed as $\mathcal{P}_{\text{meas}}$ – $(dk/dt)_{meas}$. A weighting factor W is selected such that the magnitude of both terms in Eq. 11 are approximately equal. Despite this weighting, the sum over the error in k varies most rapidly and dominates the changes that occur in F. It transpires, however, that both sums are minimized by similar values of C_3, and neither the precise value of W nor the dominance of the error in k is of great concern.

5) The model predictions of k and ε, particularly k, are sensitive to initial conditions. Estimates of appropriate initial conditions are obtained from the experimentally determined k, and from an estimate of the dissipation obtained using the relation

$$\varepsilon = A \frac{\left(\tfrac{2}{3}k\right)^{3/2}}{\ell} \qquad (12)$$

Measurements obtained in isotropic grid turbulence [21] suggest $A = 0.55$. To evaluate the suitability of this value of A to engine flows, we have computed the mean square error between the measured shear stress $u_r u_\theta$ and that computed via Eq. 5, using the measured k, ℓ and $S_{r\theta}$, for various values of A:

$$Error = \sum \left(u_r u_\theta + \frac{2C_\mu}{A} \frac{k^{1/2}\,\ell}{\left(\tfrac{2}{3}\right)^{3/2}} S_{r\theta} \right)^2 \qquad (13)$$

The summation is taken over data obtained at all operating conditions and crank angles. Figure 4 shows that the minimum error is obtained with $A \approx 0.6$.

Uncertainty in the initial kinetic energy can be introduced by anisotropy. That is, the unmeasured axial normal stress u_z^2 may differ significantly from $\tfrac{1}{2}\left(u_r^2 + u_\theta^2\right)$, the estimate implicit in Eq. (7). Taking the difference in the measured normal stresses from $\tfrac{1}{2}\left(u_r^2 + u_\theta^2\right)$ as a measure of the likely uncertainty in u_z^2, a $\pm 2\sigma$ uncertainty in k of ±8.5% is

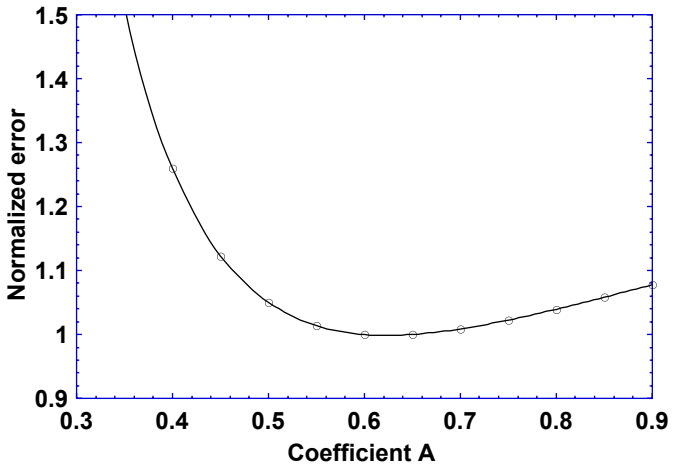

Figure 4 Mean square error, computed via Eq. 13, incurred in estimating the shear stress $u_r u_\theta$ with Eq. 5.

estimated. The uncertainty in ε is less easily found, due to the difficulty of quantifying uncertainties in ℓ and A. Accordingly, an uncertainty of 30% is selected as a reasonable estimate.

The minimization of F is pursued allowing the initial conditions on k and ε to vary within their respective uncertainties from the nominal values deduced from the measured estimate of k and from Eq. 12. When initial conditions were allowed to vary the initial k was usually higher and initial ε was usually lower. The "best" C_3 obtained was invariably smaller, typically by about 10%.

6) Minimization of Eq. 11 was performed with fixed values for C_1 and C_2 of 1.44 and 1.92, respectively.

RESULTS AND DISCUSSION

Table 3 summarizes the optimal values of the constant C_3 obtained at each measurement location for each of the three swirl ratios investigated. A mean value of 1.75 is obtained, with a spread in observed values of approximately ±0.27. The mean value lies close to El Tahry's [5] theoretical recommendation of 1.58 and the recommendation of Ikegami *et al.* [14] of 1.7 for use during compression. There is no significant correlation observed between the values of C_3 and either measurement location or swirl ratio. Hence, the estimates of C_3 appear insensitive to both the degree of flow inhomogeneity and the relative importance of the

Table 3 Values obtained for the constant C_3

	R_s = 1.5	R_s = 2.5	R_s = 3.5
z = 4 mm	1.62	1.92	1.71
z = 8 mm	1.90	1.54	1.49
z = 12 mm	1.72	2.03	1.82

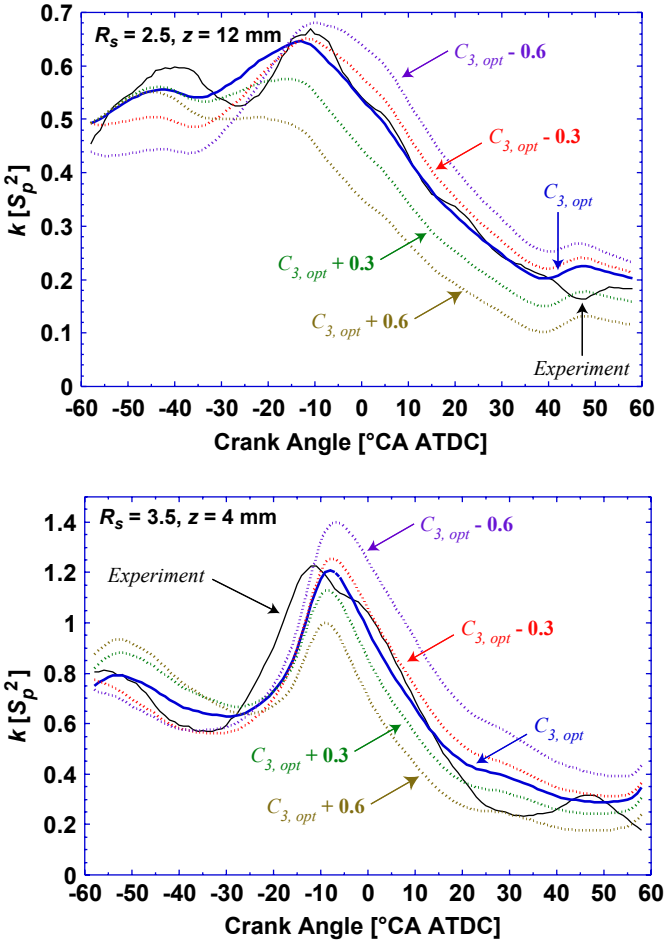

Figure 5 Comparison of model predictions with measurements of k for two selected data sets.

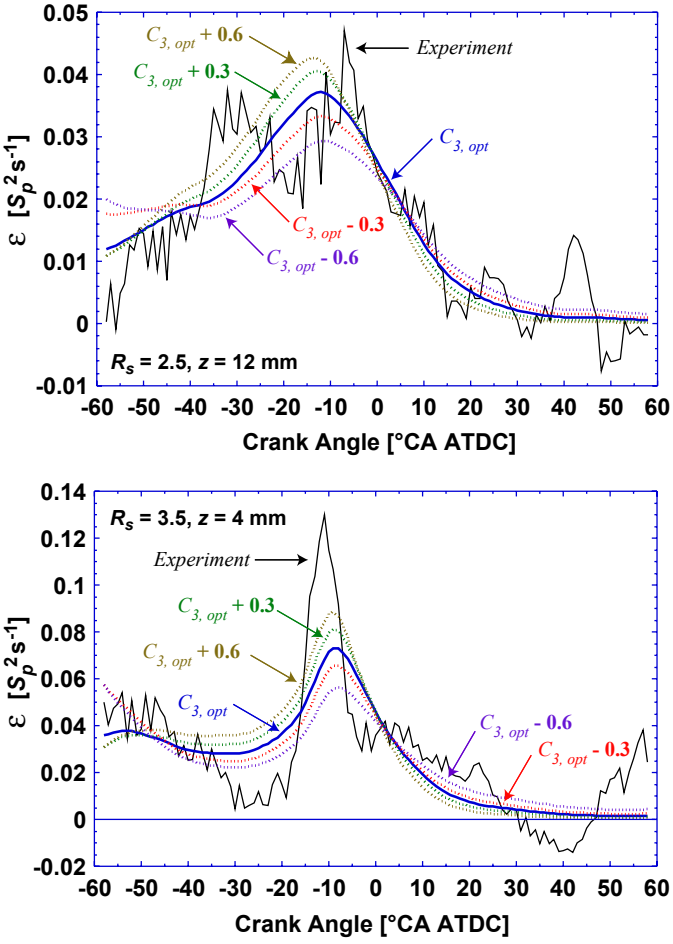

Figure 6 Comparison of model predictions with measurements of ε for two selected data sets.

anisotropic stresses and production associated with these stresses.

The quality of the model predictions of k can be assessed from Fig. 5, which compares the measured k to the predictions of Eqs. 2 and 3 using the optimal value found for C_3. The comparison is made for two selected data sets, one corresponding to a location and swirl ratio where turbulence is dominated by $\mathcal{P}_{iso}$ (R_s = 2.5 and z = 12 mm) and the other to a location and swirl ratio where production associated with the anisotropic stresses is dominant prior to TDC (R_s = 3.5 and z = 4 mm). Overall, the model predicts the measured k well. During the expansion stroke, however, the optimal value of C_3 tends to result in over-prediction of k. This behavior is typical of the majority of the data analyzed.

Also shown in Fig. 5 are the model predictions for values of C_3 corresponding to approximately *1x* and *2x* the spread observed in Table 3. For these non-optimal simulations, the initial conditions were allowed to vary within the prescribed bounds in order to obtain the best possible fit. For the lower swirl ratio, the results shown in the upper portion of Fig. 5 show that the kinetic energy computed using the optimal value determined for C_3 provides an unambiguously superior fit to the measured evolution of k. For the higher swirl ratio, the fit achieved with C_3 deviating ±0.6 from the optimum is plainly inferior, under-predicting the turbulence energy over the bulk of the cycle when C_3 is too large and over-predicting the energy when C_3 is too small. However, with smaller deviations of ±0.3, during significant portions of the record the fit to the non-optimal model predictions can be better than the fit obtained when an optimal value of C_3 is employed. Based on this behavior, and the spread of values observed in Table 3, it seems reasonable to assign a value of ±0.3 as a rough measure of the uncertainty in C_3.

Model predictions of the evolution of ε are shown in Fig. 6. Although the experimental estimates of ε exhibit significantly greater fluctuations than the estimates of k, it is clear that the model predictions capture the general trends well. In the low swirl case, where flow inhomogeneities are expected to be less pronounced, the fit is quite good. Nevertheless, inspection of the fit to several data sets leads to the general observation that the dissipation is often underestimated by the model during the expansion stroke—in a manner similar to that seen in the lower portion of Fig. 6 for the higher swirl ratio.

The model predictions in Fig. 6 obtained for different values of C_3 clearly exhibit the influence of C_3 on ε. When C_3 is too large, the dissipation is too high during

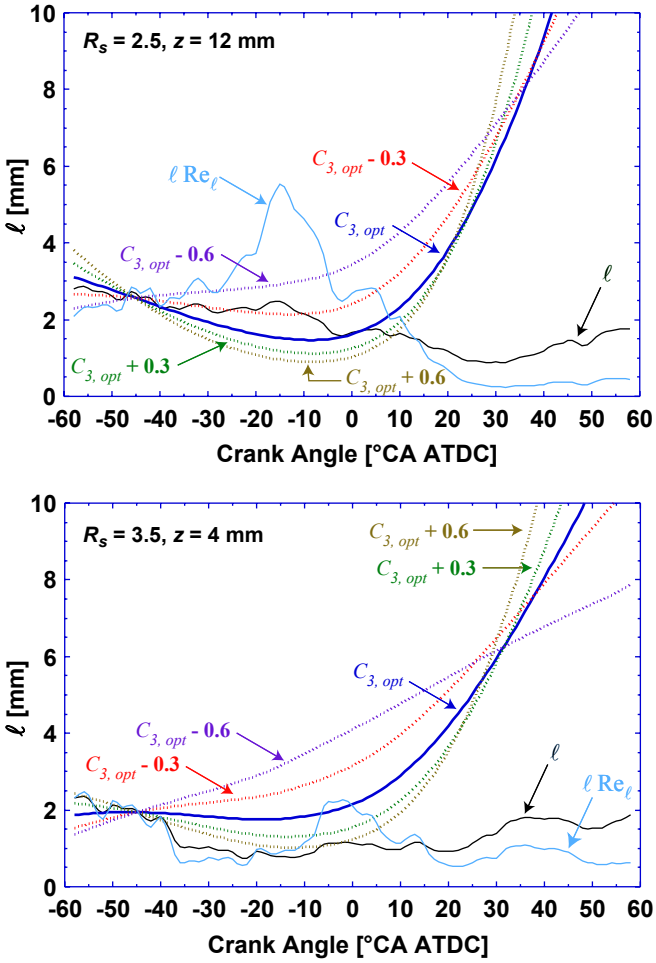

Figure 7 Comparison of model predictions with measurements of ℓ for two selected data sets.

compression ($\nabla\cdot\mathbf{U} < 0$) and too low during expansion ($\nabla\cdot\mathbf{U} > 0$). The converse is true when C_3 is too small. Note further that the initial value of ε, which is subject to greater uncertainty than the initial value of k, does not significantly influence the behavior of ε over the majority of the record.

The behavior of the model length scale ℓ_ε is compared to the velocity-correlation length scale ℓ in Fig. 7, for the same data sets presented in Figs. 5 and 6. Also shown in Fig. 7 is the quantity $\ell\mathrm{Re}_\ell$. As noted earlier, ℓ_ε is expected to scale with $\ell\mathrm{Re}_\ell$ under conditions of rapid distortion. The values of ℓ_ε and $\ell\mathrm{Re}_\ell$ have been scaled such that their average values from -50 to -40°CA match the average value of ℓ.

Although the viscosity ν decreases by a factor of approximately 3.5 during the last 60°CA of compression and turbulence levels typically are increasing, the ℓ^2 dependence of $\ell\mathrm{Re}_\ell$ can often dominate, and $\ell\mathrm{Re}_\ell$ may decrease during compression. Generally, however, it increases during compression and decreases during expansion.

At the lower swirl ratio, the model length scales corresponding to the larger values of C_3 follow the observed (and anticipated) trends in ℓ, decreasing as TDC is approached. The modest experimental decrease is best matched by the behavior of ℓ_ε when the optimal value of C_3 or a somewhat lower value is used. Note that even the smallest value of C_3 investigated falls within the bounds provided by $\ell\mathrm{Re}_\ell$. Contrasting behavior is seen at higher swirl, however. In this case, the evolution of both ℓ and $\ell\mathrm{Re}_\ell$ are best matched with the optimal and larger values of C_3. Overall, the behavior of the length scale during compression does not support the use of a value of C_3 other than the optimal value determined by minimizing Eq. 11.

During expansion, all model scales are observed to increase rapidly, behavior which is not seen in either ℓ or $\ell\mathrm{Re}_\ell$. Small values of C_3 lead to a smaller rate of increase of ℓ_ε. Some insight into this behavior can be obtained by differentiating $\ell_\varepsilon = k^{3/2}/\varepsilon$ and employing homogeneous flow approximations for Eqs. 2 and 3:

$$\frac{1}{\ell_\varepsilon}\frac{d\ell_\varepsilon}{dt} = \left(\frac{3}{2} - C_1\right)\frac{\mathcal{P}}{k} + (C_2 - \frac{3}{2})\frac{\varepsilon}{k} - (1 - C_3)(\nabla\cdot\mathbf{U}) \quad (14)$$

For standard values of the coefficients C_1 and C_2, the multipliers of the first two terms on the RHS are small but positive. The second term leads to the growth in length scale observed in decaying, incompressible grid turbulence. If we wish to restrict the growth in length scale during expansion to similar levels, the first and last terms must sum to approximately zero. $\mathcal{P}$ is typically bounded by $\mathcal{P}_{iso}$ during expansion. Hence the sum of these terms can be written

$$\left(\frac{3}{2} - C_1\right)\left(-\frac{2}{3}(\nabla\cdot\mathbf{U})\right) - (1 - C_3)(\nabla\cdot\mathbf{U}) \approx 0 \quad (15)$$

From Eq. 15 we find that plausible length scale behavior during expansion requires $C_3 \approx 1$. However, values of C_3 this small result in unrealistic increases in ℓ_ε during compression and, as seen in Figs. 5 and 6, lead to significant errors in the modeling of k and ε. A conclusion which can be drawn from these observations is that no single value of C_3 can be found that provides satisfactory modeling of k, ε, and ℓ during both compression and expansion. Nevertheless, no compelling argument can be made for adopting a particular value for C_3 other than that which was found to be optimal for modeling k and ε.

The above conclusion does not imply that the model length scale is a faulty representation of the velocity correlation length scale. Rather, when a single value of C_3 is employed, the modeling errors are more apparent during expansion, where we have above observed a general tendency to overestimate k and underestimate ε. Both of these behaviors are consistent with over-prediction of the length scale during expansion. When the analysis of the experimental data is restricted to the expansion stroke, a mean optimal value for C_3 of just 0.9 is found, and the model length scale behavior tracks that of ℓ more closely.

A similar exercise, restricting the analysis to just the compression stroke, has only a small influence on the

optimal value of C_3, reducing the mean value obtained to 1.67. The lower value of C_3 results in somewhat higher levels of k, which are forced lower during compression when all crank angles are considered to avoid errors caused by the underestimation of ε that occurs during expansion.

Adopting a value for C_3 that varies throughout the cycle is not necessarily problematic. Strain-rate/time-scale dependent formulations, such as that of Han and Reitz [9], have the potential to capture this behavior without adding significant additional computational complexity. Our future work will evaluate the ability of this model to capture the required behavior of C_3.

A potential source of uncertainty in our evaluation of the best single value of C_3 for use in modeling engine flows—which has not yet been addressed—arises from the well-worn question of the influence of cyclic variability on our measured turbulence statistics. Experimental estimation of the mean velocity gradients is anticipated to be relatively unaffected by random cycle-to-cycle fluctuations in bulk flow structures. However, the various components of the turbulent stresses (as well as k) could be significantly overestimated. Several arguments can be mustered to suggest that cycle-to-cycle variations do not present a serious problem in this study. Swirling flows, and flows that are strongly directed by combustion chamber geometry, are anticipated to be less susceptible to cycle-to-cycle fluctuations [22,23]. Additionally, the anisotropic stresses measured in these flows can be very successfully modeled using models developed and optimized for canonical laboratory flows [13]. Nevertheless, to investigate the influence of this potential error the measured stresses have been assumed to be overestimated by 50%. Consequently, from Eq. 4, the production is similarly overestimated. Adjusting k and $\mathcal{P}$ accordingly, the "best fit" values for C_3 obtained vary approximately ±0.25 about a mean of 1.89. Hence, the optimal value identified for C_3 is unlikely to be appreciably influenced by experimental overestimation of the stresses. Significantly, the fit to k provided by Eq. 2 is considerably poorer when the stresses are assumed to be overestimated, as is shown in Fig. 8. If the turbulence modeling embodied in Eqs. 2 and 3 has general applicability, then the poor agreement obtained when the experimental stresses are assumed to be overestimated suggests that any such overestimation is minor.

CONCLUSIONS

- A mean "best-fit" value of C_3 of 1.75 is found for crank angles between -50 and 50°CA ATDC, with a spread in observed values of approximately ±0.27.
- Estimates of C_3 are insensitive to both the degree of flow inhomogeneity and the relative importance of the anisotropic stresses and production associated with these stresses.

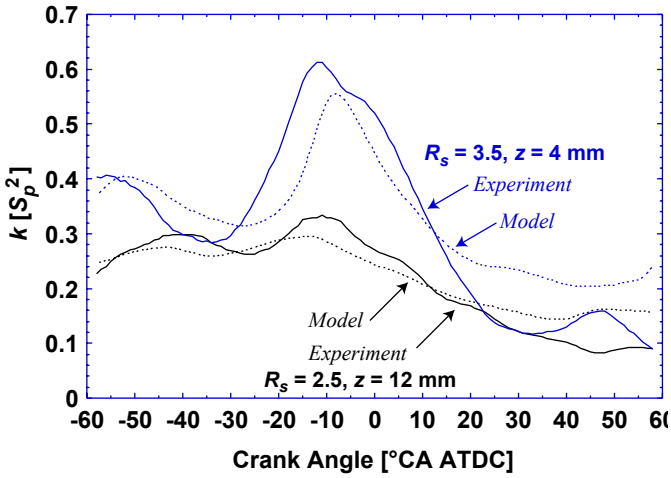

Figure 8 Comparison of model predictions to measurements of k for the data sets of Fig. 5, using the value of C_3 that provided the best fit to the data assuming that the measured stresses have been overestimated by 50%.

- Overall, the model predicts the measured k and ε well—though k tends to be over-predicted and ε under-predicted during the expansion stroke. The model length scale $k^{3/2}/\varepsilon$ grows too rapidly during expansion when a single, "best-fit" value of C_3 is used.
- No single value of C_3 can be found such that k, ε, and ℓ are accurately modeled during both compression and expansion.
- The model length scale generally evolves in a similar manner to the velocity correlation length scale when a value of C_3 is employed that allows a good *local* prediction of k and ε.
- The above conclusions are not strongly affected by errors in the measured turbulent stresses caused by cycle-to-cycle fluctuations in mean flow structure.

ACKNOWLEDGMENTS

Support for this research was provided by the U.S. Department of Energy, Office of FreedomCAR and Vehicle Technologies. The research was performed at the University of Wisconsin (Madison) Engine Research Center and at the Combustion Research Facility of Sandia National Laboratories. Sandia is a multiprogram laboratory operated by Sandia Corporation, a Lockheed Martin Company, for the United States Department of Energy's National Nuclear Security Administration under contract DE-AC04-94AL85000.

References

1. Gosman AD, Johns RJR, and Watkins AP. "Development of Prediction Methods for In-Cylinder Processes in Reciprocating Engines," *in* Combustion Modeling in Reciprocating Engines, Mattavi JN and Amann CA, *eds*. Plenum Press, 1980.

2. Reynolds WC. “Modeling of Fluid Motions in Engines—An Introductory Overview,” *in* Combustion Modeling in Reciprocating Engines, Mattavi JN and Amann CA, *eds*. Plenum Press, 1980.

3. Ramos JI and Sirignano WA. “Axisymmetric Flow Model with and without Swirl in a Piston Cylinder Arrangement with Idealized Valve Operation, SAE Paper No. 800284, 1980.

4. Morel T and Mansour NN. “Modeling of Turbulence in Combustion Engines,” SAE Paper No. 820040, 1982.

5. El Tahry SH. “*k-ε* Equation for Compressible Reciprocating Engine Flows,” *J. Energy* **4**:345-353, 1983.

6. Grasso F and Bracco FV. “Computed and Measured Turbulence in Axisymmetric Reciprocating Engines,” *AIAA J.* **21**:601-607, 1983.

7. Amsden AA, O’Rourke PJ, and Butler, TD. “KIVA-II: A Computer Program for Chemically Reactive Flows with Sprays,” Los Alamos National Laboratory Report LA-11560-MS, 1989.

8. Coleman GN and Mansour NN. “Modeling the Rapid Spherical Compression of Isotropic Turbulence,” *Phys. Fluids* **3**:2255-2259, 1993.

9. Han Z and Reitz RD. “Turbulence Modeling of Internal Combustion Engines Using RNG *k-ε* Models,” *Combust. Sci. and Tech.* **106**:267-295.

10. Bianchi GM, Michelassi V, and Reitz RD. ‚Modeling the Isotropic Turbulence Dissipation in Engine Flows by Using the Linear *k-ε* Model,” Proc. of the ICE Division of ASME: Fall Technical Conference, Ann Arbor, MI, 16-20 October, 1999.

11. Ahmadi-Befrui B, Gosman AD, Lockwood FC, and Watkins AP. “Multidimensional Calculation of Combustion in an Idealised Homogeneous Charge Engine: a progress Report,” SAE Paper No. 810151, 1981.

12. Funk C, Sick V, Reuss DL, and Dahm JA. “Turbulence Properties of High and Low Swirl In-Cylinder Flows,” SAE Paper No. 2002-01-2841, 2002.

13. Miles PC. “In-Cylinder Turbulent Flow Structure in Direct-Injection, Swirl-Supported Diesel Engines,” *in* Flow and Comb. in Automotive Engines, C. Arcoumanis, ed. Springer-Verlag (*In Press*).

14. Ikegami M, Shioji M, and Nishimoto K. “Turbulence Intensity and Spatial Integral Scale During Compression and Expansion Strokes in a Four-Cycle Reciprocating Engine,” SAE Paper No. 870372, 1987.

15. Fraser RA and Bracco FV. “Cycle-Resolved LDV Integral Length Scale Measurements Investigating Clearance Height Scaling, Isotropy, and Homogeneity in an I.C. Engine,” SAE Paper No. 890615, 1989.

16. Han Z, Reitz RD, Corcione FE, and Valentino G. “Interpretation of *k-ε* Computed Length-Scale Predictions for Engine Flows,” Proc. 26th Symposium (Int’l.) on Combustion, Naples, Italy, July 28 – August 2, 1996.

17. Miles PC, Megerle M, Nagel Z, Reitz RD, Lai M-C, and Sick V. “An Experimental Assessment of Turbulence Production, Reynolds Stress, and Length Scale (Dissipation) Modeling in a Swirl-Supported DI Diesel Engine,” SAE Paper No. 2003-01-1072, 2003.

18. Wu C-T, Ferziger JH, and Chapman DR. “Simulation and Modeling of Homogeneous Compressed Turbulence,” Stanford University Department of Mechanical Engineering Thermosciences Division Report TH-21, 1985.

19. Miles P, Choi D, Megerle M, RempelEwert B, Reitz RD, Lai M-C, and Sick V. “The Influence of Swirl Ratio on Turbulent Flow Structure in a Motored HSDI Diesel Engine—A Combined Experimental and Numerical Study,” SAE Paper No. 2004-01-1678, 2004.

20. Coleman GN and Mansour NN. “Simulation and Modeling of Homogeneous Compressible Turbulence Under Isotropic Mean Compression,” Turbulent Shear Flows 8, pp.269-281, Springer-Verlag, 1993.

21. Comte-Bellot G and Corrsin S. “Simple Eulerian Time Correlation of Full- and Narrow-band Velocity Signals in Grid-Generated, ‘Isotropic’ Turbulence,” *J. Fluid Mech.* **48**:273-337, 1971.

22. Rask RB. “Comparison of Window, Smoothed-Ensemble, and Cycle-by-Cycle Data Reduction Techniques for Laser Doppler Anemometer Measurements of In-Cylinder Velocity.” In: Proc ASME symposium on fluid mechanics of combustion systems, June 22-23, Boulder, Colorado, 1981.

23. Liou T-M, Santavicca DA. “Cycle resolved turbulence measurements in a ported engine with and without swirl.” SAE Paper No. 830419, 1983.

24. Jakirlić S, Tropea C, Hadžić I, Pascal H, Hanjalić K. “Computational Study of Joint Effects of Shear, Compression and Swirl on Flow and Turbulence in a Valve-less Piston-Cylinder Assembly.” SAE Paper No. 2001-01-1236, 1983.